Passive mode locking of ytterbium- and erbium-doped all-fiber lasers using graphene oxide saturable absorbers

Hou-Ren Chen,[1] Chih-Ya Tsai,[1] Hsin-Ming Cheng,[2] Kuei-Huei Lin,[3,4] and Wen-Feng Hsieh[1,*]

[1]*Department of Photonics & Institute of Electro-Optical Engineering, National Chiao Tung University, 1001, Ta-Hsueh Rd., Hsinchu 300, Taiwan*
[2]*Material and Chemical Research Laboratories, Industrial Technology Research Institute, Hsinchu 310, Taiwan*
[3]*Department of Applied Physics and Chemistry, University of Taipei, 1, Ai-Guo West Rd., Taipei 100, Taiwan*
[4]*khlin@utaipei.edu.tw*
[*] *wfhsieh@mail.nctu.edu.tw*

Abstract: Broadband graphene oxide/PVA films were used as saturable absorbers (SAs) for mode locking erbium-doped fiber laser (EDFL) and ytterbium-doped fiber laser (YDFL) at 1.06 μm and 1.55 μm. They provide modulation depths of 3.15% and 6.2% for EDFL and YDFL, respectively. Stable self-starting mode-locked pulses are obtained for both lasers, confirming that the graphene oxide is cost-effective. We have generated mode-locked pulses with spectral width, repetition rate, and pulse duration of 0.75 nm, 9.5 MHz, and 2.7 ps. This is the shortest pulse duration directly obtained from an all-normal-dispersion YDFL with graphene-oxide saturable absorber.

OCIS codes: (140.3500) Lasers, erbium; (140.3510) Lasers, fiber; (140.4050) Mode-locked lasers; (160.4330) Nonlinear optical materials; (140.3615) Lasers, ytterbium.

References and links

1. U. Keller, K. J. Weingarten, F. X. Kartner, D. Kopf, B. Braun, I. D. Jung, R. Fluck, C. Honninger, N. Matuschek, and J. A. derAu, "Semiconductor saturable absorber mirrors (SESAM's) for femtosecond to nanosecond pulse generation in solid-state lasers," IEEE J. Sel. Top. Quantum Electron. **2**(3), 435–453 (1996).
2. H. R. Chen, J. H. Lin, K. T. Song, K. H. Lin, and W. F. Hsieh, "Passive mode-locking in diode-pumped c-cut Nd:$LuVO_4$ laser with a semiconductor saturable-absorber mirror, " Appl. Phys. B. **96**(1), 19–23 (2009).
3. S. Y. Set, H. Yaguchi, Y. Tanaka, and M. Jablonski, "Laser mode locking using a saturable absorber incorporating carbon nanotubes," J. Lightwave Technol. **22**(1), 51–56 (2004).
4. F. Wang, A. G. Rozhin, V. Scardaci, Z. Sun, F. Hennrich, I. H. White, W. I. Milne, and A. C. Ferrari, "Wideband-tuneable, nanotube mode-locked, fibre laser," Nat. Nanotechnol. **3**(12), 738–742 (2008).
5. J. C. Chiu, C. M. Chang, B. Z. Hsieh, S. C. Lin, C. Y. Yeh, G. R. Lin, C. K. Lee, J. J. Lin, and W. H. Cheng, "Pulse shortening mode-locked fiber laser by thickness and concentration product of carbon nanotube based saturable absorber," Opt. Express **19**(5), 4036–4041 (2011).
6. J. C. Chiu, Y. F. Lan, C. M. Chang, X. Z. Chen, C. Y. Yeh, C. K. Lee, G. R. Lin, J. J. Lin, and W. H. Cheng, "Concentration effect of carbon nanotube based saturable absorber on stabilizing and shortening mode-locked pulse," Opt. Express **18**(4), 3592–3600 (2010).
7. F. Shohda, M. Nakazawa, J. Mata, and J. Tsukamoto, "A 113 fs fiber laser operating at 1.56 mum using a cascadable film-type saturable absorber with P3HT-incorporated single-wall carbon nanotubes coated on polyamide," Opt. Express **18**(9), 9712–9721 (2010).
8. J. C. Travers, J. Morgenweg, E. D. Obraztsova, A. I. Chernov, E. J. R. Kelleher, and S. V. Popov, "Using the E-22 transition of carbon nanotubes for fiber laser mode-locking," Laser Phys. Lett. **8**(2), 144–149 (2011).
9. Z. Sun, T. Hasan, and A. C. Ferrari, "Ultrafast lasers mode-locked by nanotubes and graphene," Physica E **44**(6), 1082–1091 (2012).
10. A. Martinez and Z. P. Sun, "Nanotube and graphene saturable absorbers for fibre lasers," Nat. Photonics **7**(11), 842–845 (2013).
11. M. A. Solodyankin, E. D. Obraztsova, A. S. Lobach, A. I. Chernov, A. V. Tausenev, V. I. Konov, and E. M. Dianov, "Mode-locked 1.93 microm thulium fiber laser with a carbon nanotube absorber," Opt. Lett. **33**(12), 1336–1338 (2008).
12. W. B. Cho, J. H. Yim, S. Y. Choi, S. Lee, U. Griebner, V. Petrov, and F. Rotermund, "Mode-locked self-starting Cr:forsterite laser using a single-walled carbon nanotube saturable absorber," Opt. Lett. **33**(21), 2449–2451 (2008).

#208911 - $15.00 USD Received 26 Mar 2014; revised 3 May 2014; accepted 8 May 2014; published 20 May 2014

13. W. B. Cho, A. Schmidt, J. H. Yim, S. Y. Choi, S. Lee, F. Rotermund, U. Griebner, G. Steinmeyer, V. Petrov, X. Mateos, M. C. Pujol, J. J. Carvajal, M. Aguiló, and F. Díaz, "Passive mode-locking of a Tm-doped bulk laser near 2 microm using a carbon nanotube saturable absorber," Opt. Express **17**(13), 11007–11012 (2009).
14. H. R. Chen, Y. G. Wang, C. Y. Tsai, K. H. Lin, T. Y. Chang, J. Tang, and W. F. Hsieh, "High-power, passively mode-locked Nd:$GdVO_4$ laser using single-walled carbon nanotubes as saturable absorber," Opt. Lett. **36**(7), 1284–1286 (2011).
15. H. Kataura, Y. Kumazawa, Y. Maniwa, I. Umezu, S. Suzuki, Y. Ohtsuka, and Y. Achiba, "Optical properties of single-wall carbon nanotubes," Synth. Met. **103**(1-3), 2555–2558 (1999).
16. P. Avouris and M. Freitag, "Graphene Photonics, Plasmonics, and Optoelectronics," IEEE J. Sel. Top. Quantum Electron. **20**(1), 600112 (2014).
17. F. Bonaccorso, Z. Sun, T. Hasan, and A. C. Ferrari, "Graphene photonics and optoelectronics," Nat. Photonics **4**(9), 611–622 (2010).
18. T. Hasan, Z. P. Sun, F. Q. Wang, F. Bonaccorso, P. H. Tan, A. G. Rozhin, and A. C. Ferrari, "Nanotube-Polymer Composites for Ultrafast Photonics," Adv. Mater. **21**(38â€“39), 3874–3899 (2009).
19. Q. L. Bao, H. Zhang, Y. Wang, Z. H. Ni, Y. L. Yan, Z. X. Shen, K. P. Loh, and D. Y. Tang, "Atomic-Layer Graphene as a Saturable Absorber for Ultrafast Pulsed Lasers," Adv. Funct. Mater. **19**(19), 3077–3083 (2009).
20. I. H. Baek, H. W. Lee, S. Bae, B. H. Hong, Y. H. Ahn, D. I. Yeom, and F. Rotermund, "Efficient Mode-Locking of Sub-70-fs Ti: Sapphire Laser by Graphene Saturable Absorber," Appl. Phys. Express **5**(3), 032701 (2012).
21. C. A. Zaugg, Z. Sun, V. J. Wittwer, D. Popa, S. Milana, T. S. Kulmala, R. S. Sundaram, M. Mangold, O. D. Sieber, M. Golling, Y. Lee, J. H. Ahn, A. C. Ferrari, and U. Keller, "Ultrafast and widely tuneable vertical-external-cavity surface-emitting laser, mode-locked by a graphene-integrated distributed Bragg reflector," Opt. Express **21**(25), 31548–31559 (2013).
22. W. D. Tan, C. Y. Su, R. J. Knize, G. Q. Xie, L. J. Li, and D. Y. Tang, "Mode locking of ceramic Nd:yttrium aluminum garnet with graphene as a saturable absorber," Appl. Phys. Lett. **96**(3), 031106 (2010).
23. Z. Q. Luo, Y. Z. Huang, J. Z. Wang, H. H. Cheng, Z. P. Cai, and C. C. Ye, "Multiwavelength Dissipative-Soliton Generation in Yb-Fiber Laser Using Graphene-Deposited Fiber-Taper," IEEE Photon. Technol. Lett. **24**(17), 1539–1542 (2012).
24. R. Mary, G. Brown, S. J. Beecher, F. Torrisi, S. Milana, D. Popa, T. Hasan, Z. P. Sun, E. Lidorikis, S. Ohara, A. C. Ferrari, and A. K. Kar, "1.5 GHz picosecond pulse generation from a monolithic waveguide laser with a graphene-film saturable output coupler," Opt. Express **21**(7), 7943–7950 (2013).
25. E. Ugolotti, A. Schmidt, V. Petrov, J. W. Kim, D. I. Yeom, F. Rotermund, S. Bae, B. H. Hong, A. Agnesi, C. Fiebig, G. Erbert, X. Mateos, M. Aguilo, F. Diaz, and U. Griebner, "Graphene mode-locked femtosecond Yb:KLuW laser," Appl. Phys. Lett. **101**(16), 161112 (2012).
26. W. B. Cho, J. W. Kim, H. W. Lee, S. Bae, B. H. Hong, S. Y. Choi, I. H. Baek, K. Kim, D.-I. Yeom, and F. Rotermund, "High-quality, large-area monolayer graphene for efficient bulk laser mode-locking near 1.25 μm," Opt. Lett. **36**(20), 4089–4091 (2011).
27. H. Zhang, D. Y. Tang, L. M. Zhao, Q. L. Bao, and K. P. Loh, "Large energy mode locking of an erbium-doped fiber laser with atomic layer graphene," Opt. Express **17**(20), 17630–17635 (2009).
28. Z. P. Sun, D. Popa, T. Hasan, F. Torrisi, F. Q. Wang, E. J. R. Kelleher, J. C. Travers, V. Nicolosi, and A. C. Ferrari, "A stable, wideband tunable, near transform-limited, graphene-mode-locked, ultrafast laser," Nano Res. **3**(9), 653–660 (2010).
29. D. Popa, Z. Sun, F. Torrisi, T. Hasan, F. Wang, and A. C. Ferrari, "Sub 200 fs pulse generation from a graphene mode-locked fiber laser," Appl. Phys. Lett. **97**, 203106 (2010).
30. Y. M. Chang, H. Kim, J. H. Lee, and Y.-W. Song, "Multilayered graphene efficiently formed by mechanical exfoliation for nonlinear saturable absorbers in fiber mode-locked lasers," Appl. Phys. Lett. **97**(21), 211102 (2010).
31. A. A. Lagatsky, Z. Sun, T. S. Kulmala, R. S. Sundaram, S. Milana, F. Torrisi, O. L. Antipov, Y. Lee, J. H. Ahn, C. T. A. Brown, W. Sibbett, and A. C. Ferrari, "2 μm solid-state laser mode-locked by single-layer graphene," Appl. Phys. Lett. **102**(1), 013113 (2013).
32. M. Zhang, E. J. R. Kelleher, F. Torrisi, Z. Sun, T. Hasan, D. Popa, F. Wang, A. C. Ferrari, S. V. Popov, and J. R. Taylor, "Tm-doped fiber laser mode-locked by graphene-polymer composite," Opt. Express **20**(22), 25077–25084 (2012).
33. M. N. Cizmeciyan, J. W. Kim, S. Bae, B. H. Hong, F. Rotermund, and A. Sennaroglu, "Graphene mode-locked femtosecond Cr:ZnSe laser at 2500 nm," Opt. Lett. **38**(3), 341–343 (2013).
34. D. Popa, Z. Sun, T. Hasan, F. Torrisi, F. Wang, and A. C. Ferrari, "Graphene Q-switched, tunable fiber laser," Appl. Phys. Lett. **98**(7), 073106 (2011).
35. Y. H. Bo Fu, Yi Hua, Xiaosheng Xiao, Hongwei Zhu, Zhipei Sun, and Changxi Yang, "Broadband Graphene Saturable Absorber for Pulsed Fiber Lasers at 1, 1.5, and 2 μm," IEEE J. Sel. Top. Quantum Electron. **20**(5), 110705 (2014).
36. F. Bonaccorso and Z. P. Sun, "Solution processing of graphene, topological insulators and other 2d crystals for ultrafast photonics," Opt. Mater. Express **4**(1), 63–78 (2014).
37. J. Xu, J. Liu, S. D. Wu, Q. H. Yang, and P. Wang, "Graphene oxide mode-locked femtosecond erbium-doped fiber lasers," Opt. Express **20**(14), 15474–15480 (2012).
38. A. Reina, X. T. Jia, J. Ho, D. Nezich, H. B. Son, V. Bulovic, M. S. Dresselhaus, and J. Kong, "Large Area, Few-Layer Graphene Films on Arbitrary Substrates by Chemical Vapor Deposition," Nano Lett. **9**(1), 30–35 (2009).

#208911 - $15.00 USD Received 26 Mar 2014; revised 3 May 2014; accepted 8 May 2014; published 20 May 2014

39. S. Stankovich, D. A. Dikin, R. D. Piner, K. A. Kohlhaas, A. Kleinhammes, Y. Jia, Y. Wu, S. T. Nguyen, and R. S. Ruoff, "Synthesis of graphene-based nanosheets via chemical reduction of exfoliated graphite oxide," Carbon **45**(7), 1558–1565 (2007).
40. Y. Shen, S. B. Yang, P. Zhou, Q. Q. Sun, P. F. Wang, L. Wan, J. Li, L. Y. Chen, X. B. Wang, S. J. Ding, and D. W. Zhang, "Evolution of the band-gap and optical properties of graphene oxide with controllable reduction level," Carbon **62**, 157–164 (2013).
41. X. Zhao, Z. B. Liu, W. B. Yan, Y. P. Wu, X. L. Zhang, Y. S. Chen, and J. G. Tian, "Ultrafast carrier dynamics and saturable absorption of solution-processable few-layered graphene oxide," Appl. Phys. Lett. **98**(12), 121905 (2011).
42. K. P. Loh, Q. L. Bao, G. Eda, and M. Chhowalla, "Graphene oxide as a chemically tunable platform for optical applications," Nat. Chem. **2**(12), 1015–1024 (2010).
43. G. Sobon, J. Sotor, J. Jagiello, R. Kozinski, M. Zdrojek, M. Holdynski, P. Paletko, J. Boguslawski, L. Lipinska, and K. M. Abramski, "Graphene Oxide vs. Reduced Graphene Oxide as saturable absorbers for Er-doped passively mode-locked fiber laser," Opt. Express **20**(17), 19463–19473 (2012).
44. Y. G. Wang, H. R. Chen, W. F. Hsieh, and Y. H. Tsang, "Mode-locked Nd: GdVO4 laser with graphene oxide/polyvinyl alcohol composite material absorber as well as an output coupler," Opt. Commun. **289**, 119–122 (2013).
45. Y. G. Wang, Z. S. Qu, J. Liu, and Y. H. Tsang, "Graphene Oxide Absorbers for Watt-Level High-Power Passive Mode-Locked Nd:$GdVO_4$ Laser Operating at 1 μm," J. Lightwave Technol. **30**(20), 3259–3262 (2012).
46. X. H. Li, Y. G. Wang, Y. S. Wang, Y. Z. Zhang, K. Wu, P. P. Shum, X. Yu, Y. Zhang, and Q. J. Wang, "All-normal-dispersion passively mode-locked Yb-doped fiber ring laser based on a graphene oxide saturable absorber," Laser Phys. Lett. **10**(7), 075108 (2013).
47. Z. B. Liu, X. Y. He, and D. N. Wang, "Passively mode-locked fiber laser based on a hollow-core photonic crystal fiber filled with few-layered graphene oxide solution," Opt. Lett. **36**(16), 3024–3026 (2011).
48. M. Jung, J. Koo, P. Debnath, Y. W. Song, and J. H. Lee, "A Mode-Locked 1.91 μm Fiber Laser Based on Interaction between Graphene Oxide and Evanescent Field," Appl. Phys. Express **5**(11), 112702 (2012).
49. Y. G. Wang, H. R. Chen, X. M. Wen, W. F. Hsieh, and J. Tang, "A highly efficient graphene oxide absorber for Q-switched Nd:$GdVO_4$ lasers," Nanotechnology **22**(45), 455203 (2011).
50. G. Eda and M. Chhowalla, "Chemically Derived Graphene Oxide: Towards Large-Area Thin-Film Electronics and Optoelectronics," Adv. Mater. **22**(22), 2392–2415 (2010).
51. S. Davide Di Dio Cafiso, E. Ugolotti, A. Schmidt, V. Petrov, U. Griebner, A. Agnesi, W. B. Cho, B. H. Jung, F. Rotermund, S. Bae, B. H. Hong, G. Reali, and F. Pirzio, "Sub-100-fs Cr:YAG laser mode-locked by monolayer graphene saturable absorber," Opt. Lett. **38**(10), 1745–1747 (2013).
52. M. L. Dennis and I. N. Duling, "Experimental Study of Sideband Generation in Femtosecond Fiber Lasers," IEEE J. Quantum Electron. **30**(6), 1469–1477 (1994).
53. A. Chong, J. Buckley, W. Renninger, and F. Wise, "All-normal-dispersion femtosecond fiber laser," Opt. Express **14**(21), 10095–10100 (2006).
54. A. Chong, W. H. Renninger, and F. W. Wise, "Properties of normal-dispersion femtosecond fiber lasers," J. Opt. Soc. Am. B **25**(2), 140–148 (2008).
55. K. Ozgören and F. O. Ilday, "All-fiber all-normal dispersion laser with a fiber-based Lyot filter," Opt. Lett. **35**(8), 1296–1298 (2010).
56. L. M. Zhao, D. Y. Tang, X. A. Wu, and H. Zhang, "Dissipative soliton generation in Yb-fiber laser with an invisible intracavity bandpass filter," Opt. Lett. **35**(16), 2756–2758 (2010).
57. Z. Sun, A. G. Rozhin, F. Wang, T. Hasan, D. Popa, W. O'Neill, and A. C. Ferrari, "A compact, high power, ultrafast laser mode-locked by carbon nanotubes," Appl. Phys. Lett. **95**(25), 253102 (2009).
58. M. E. V. Pedersen, E. J. R. Kelleher, J. C. Travers, Z. Sun, T. Hasan, A. C. Ferrari, S. V. Popov, and J. R. Taylor, "Stable Gain-Guided Soliton Propagation in a Polarized Yb-Doped Mode-Locked Fiber Laser," IEEE Photonics J. **4**(3), 1058–1064 (2012).
59. X. L. Tian, M. Tang, P. P. Shum, Y. D. Gong, C. L. Lin, S. N. Fu, and T. S. Zhang, "High-energy laser pulse with a submegahertz repetition rate from a passively mode-locked fiber laser," Opt. Lett. **34**(9), 1432–1434 (2009).
60. Y. S. Fedotov, S. M. Kobtsev, R. N. Arif, A. G. Rozhin, C. Mou, and S. K. Turitsyn, "Spectrum-, pulsewidth-, and wavelength-switchable all-fiber mode-locked Yb laser with fiber based birefringent filter," Opt. Express **20**(16), 17797–17805 (2012).
61. Z. X. Zhang, Z. W. Xu, and L. Zhang, "Tunable and switchable dual-wavelength dissipative soliton generation in an all-normal-dispersion Yb-doped fiber laser with birefringence fiber filter," Opt. Express **20**(24), 26736–26742 (2012).

1. Introduction

Ultrafast fiber lasers operating in the near infrared range have become one of the most active fields in laser research because of the wide and significant applications in industry, military and basic science. Although semiconductor saturable absorber mirrors (SESAMs) have been mostly used in laser resonators to generate mode-locked laser pulses [1, 2], they are expensive, complicated in fabrication processes, and narrow in wavelength tuning range. In recent years, both single-walled carbon nanotubes (SWCNTs) and graphene are widely

#208911 - $15.00 USD Received 26 Mar 2014; revised 3 May 2014; accepted 8 May 2014; published 20 May 2014

investigated due to their various advantages, such as fast recovery time, large saturable absorption, and ease of fabrication. Chronologically, SWCNT was first used as an effective SA at 1.55 μm [3]. The saturable absorption effect is observed in semiconductor type SWCNTs. After that, SWCNTs have been widely applied for mode locking fiber lasers [3–11] and solid-state lasers [12–14]. Because the energy band gap strongly depends on nanotube's diameter [15], it is required to precisely control the CNT diameter to tune the absorption band of CNT SAs for mode locking laser at a specific wavelength. However, broadband CNT-SAs can be made in use of different diameters and chiralities of nanotubes, e.g., Wang et al. [4] extend the operation bandwidth to 300 nm.

Graphene is superior to SWCNTs in broadband saturable absorption due to its gapless linear dispersion of Dirac electrons [16, 17]. Since the demonstrations of mode-locked lasers using graphene as SAs [18, 19], the extremely broad and flat absorption spectrum of graphene [16] allows the researchers to generate passively mode-locked laser pulses over the whole (near 1 μm to 2 μm) IR wavelength. For example, graphene-based passive mode-locking have been demonstrated for sub-70-fs Ti:sapphire laser near 800 nm [20], vertical-external-cavity surface-emitting mode-locked laser from 935 to 981 nm [21], solid-state laser and fiber laser near 1 μm [22–25], 1.25 μm [26], 1.55 μm [19, 27–30], 2 μm [31, 32], and 2.5 μm [33]. In addition, the broadband operation [28, 34] and three-wavelength operation (1 μm, 1.5 μm, and 2 μm) [35] of graphene saturable absorbers have been demonstrated. Detailed review of CNT-SAs and graphene-SAs can be found in Refs [9, 10, 36]. Although graphene possesses the broadband wavelength-independent saturable absorption, it has a small absorption of only 2.3% and a low modulation depth ~0.75% at 1060 nm [25]. The small modulation depth might not be enough to suppress continuous-wave components [37] for mode-locked pulses in high gain laser system (e.g., Yb-doped fiber laser system).

There are various methods for preparing high-quality graphene, such as chemical vapor deposition (CVD) [38] and chemical reduction method [39]. The first step of chemical reduction method is to synthesize graphene oxide from natural graphite powder. Then reduced graphene oxide (rGO) nanosheet can be obtained from graphene oxide by chemical methods using reductants such as hydrazine, dimethylhydrazine. Therefore, graphene oxide (GO) is the precursor for rGO, and it has also been widely investigated for its physical and chemical characteristics. Different from graphene, GO has strong hydrophilic and water solubility due to presence of oxygen-containing functional groups. The solubility offers superior flexibility and processibility for large-scale production of GO based optoelectronics. For example, we can fabricate graphene-oxide membrane on different kinds of substrates by a spin-coater. Although the oxygen functional groups destroy the gapless linear dispersion of Dirac electrons in graphene and make the graphene oxide (GO) insulating, the GO also possesses continuous absorbance curve with almost constant from 0.8 μm to 25 μm [40]. In addition, GO has a fast energy relaxation of hot carriers and strong saturable absorption, which is comparable to those of graphene [41, 42]. Therefore, GO has potential use as broadband SAs like graphene. Sobon et al. demonstrated that GO could be used as an efficient SA to generate sub-femtosecond Er-doped fiber laser without the need of reduction to rGO [43]. Taking into account the simpler manufacturing technology and its properties, GO seems to be a good candidate as a cost-effective saturable absorber for pulsed fiber lasers.

Recently, graphene oxide saturable absorbers (GOSAs) have been used to generate passively mode-locked pulses in diode-pumped solid-state lasers and fiber lasers at 1 μm [44–46], as well as in fiber lasers near 1.5 μm [37, 43, 47] and 2 μm [48]. Li et al. [46] report the all-normal-dispersion passively mode-locked ytterbium-doped fiber laser (YDFL) using a GO/PVA-SAs, but the shortest pulse duration they obtained was quite long of ~191 ps. Nevertheless, the pulsewidth is shorter than that of 6.5 ns using graphene as SAs in YDFL [35]. The modulation depth of GOSAs can be easily changed by varying GO concentration and thickness of GO film. Although GO have been demonstrated for passive mode-locking at different wavelength, it has not been demonstrated for broadband operation as graphene-SAs [28]. Promising results show that GO is a good candidate as saturable absorber. However, there are neither reports on GOSA mode-locked all-normal-dispersion fiber lasers at 1 μm

#208911 - $15.00 USD Received 26 Mar 2014; revised 3 May 2014; accepted 8 May 2014; published 20 May 2014

with direct few-picosecond pulse output, nor mode-locking operation covering both 1.06-μm and 1.55-μm using the same GOSA sample.

In this paper, stable and self-starting passively mode-locked fiber lasers operating at 1.06-μm (YDFL) and 1.55-μm (EDFL) are demonstrated utilizing a GO/PVA film as the saturable absorber (GO/PVA-SA). It is revealed that the same GO/PVA-SA sample can be used in both EDFL and YDFL to obtain stable and self-starting mode-locked laser pulses, which show that GOSAs can be used for broadband applications. In addition, by inserting a birefringent filter (Lyot filter) in the YDFL cavity, we obtained the spectral width, repetition rate and pulse duration of 0.75 nm, 9.5 MHz and 2.7 ps. The output pulse duration is obviously shorter than previous reports using graphene (~6.5 ns) [35] and GO (~191 ps) [46] as the SAs. To our best knowledge, this is the shortest pulse duration directly obtained from an all-normal-dispersion YDFL with GOSA.

2. Characterization of graphene oxide saturable absorbers

The GO nanosheets used in this experiment were prepared through a modified Hummers method from expanded acid-washed graphite flakes having mean thickness of less than 3 nm and diameter of 0.1 ~5.0 μm. The detailed preparation of GO/PVA-SAs can be found in Ref [49]. The GO/PVA-SA with thickness of about 3 μm can be directly cut and inserted into the all-fiber cavity between two fiber connectors. This way is more convenient and flexible than that in Refs [37, 43, 47]. In [47], Liu et al. filled the few-layered GO solution in the hollow-core photonic crystal fiber, whereas in [37] and [43], Xu et al. and Sobon et al. deposited the GO on the broadband reflective mirror and fused silica windows. Figures 1(a)–1(d) show the Raman spectrum, linear transmission, and nonlinear transmission curves of the GO/PVA-SAs. The Raman spectrum [Fig. 1(a)] was obtained with a 532-nm laser excitation. The two prominent peaks at 1349 cm^{-1} and 1601 cm^{-1} are assigned to D and G bands, respectively. The D peak is due to the defect-induced breathing mode of sp^2 rings. The G peak corresponds to optical E_{2g} photons at the Brillouin zone center and is due to bond stretching of sp^2 carbon pairs in both rings and chains [50]. A weak and broad 2D peak at 2697 cm^{-1} was found, which indicates that there was rare graphene in the GO/PVA-SA. In addition, a peak at 2954 cm^{-1} was observed, which is from PVA films [29]. The transmission spectra of GO/PVA-SA and pure PVA film were shown in Fig. 1(b) measured by a UV-visible-NIR spectrophotometer (Hitachi U4100). The transmission of PVA film is almost flat with the transmittance of 93%. However, the transmission spectrum of GO/PVA-SA shows the monotonic wavelength-dependence in the spectral range from 800 nm to 2000 nm, which is a typical feature of GO and is similar to Refs [45] and [43]. It is caused by the oxygen-containing functional groups, which have larger absorption at short wavelength. The transmittance is 62.2% and 71.8% at 1064 nm and 1560 nm, respectively. In order to determine the modulation depth, we have measured the power-dependent transmission of GO/PVA-SA at various incident powers using a 1.55-μm probe laser with ~600-fs pulsewidth and 78-MHz repetition rate [Fig. 1(c)], and a 1.06-μm laser with ~500-fs pulsewidth and 40-MHz repetition rate [Fig. 1(d)]. The GO/PVA-SA has the ability of pulse shaping due to its nonlinear absorption property. The single-pass optical transmittance of GO/PVA-SA, T(I), can be expressed as $T(I) = \exp(-[\alpha(I) + \alpha_{ns}]L)$, where L, α(I), and α_{ns} are the thickness, nonlinear absorption coefficient and non-saturable absorption coefficient of GO/PVA-SA, respectively. The intensity dependence of α(I) is given by $\alpha(I) = \alpha_0(1 + 1/I_{sat})^{-1}$, where $\alpha_0 = \sigma N$ and $I_{sat} = \hbar\omega_l / \sigma\tau$ are the linear absorption coefficient and saturation intensity, respectively. Here σ, N, ω_l, and τ are the absorption cross-section of GO/PVA-SA, concentration of GO/PVA-SA, laser frequency, and energy relaxation time of GO/PVA-SA. By fitting the absolute transmittance of the GO/PVA-SA versus the input intensity, we obtained the saturation intensity I_{sat} ≈65 MW/cm^2, and the modulation depth (ΔT) is about 3.15% at 1560 nm. Similarly, the saturation intensity is about 108 MW/cm^2 and ΔT is about 6.2% at 1064 nm. Assume there is not much difference in the values of σ and τ at 1060 nm and 1550 nm due to flat dispersion of GO, we have the larger I_{sat} at the short wavelength,

#208911 - $15.00 USD Received 26 Mar 2014; revised 3 May 2014; accepted 8 May 2014; published 20 May 2014

consistent with the experimental results of decreasing ΔT (modulation depth) of GO/PVA-SA with wavelength. Similar result can be found for graphene-SAs [51]. The measured I_{sat} ≈65 MW/cm^2 and ΔT ≈3.15% are comparable with those of 60 MW/cm^2 and 2.6% in Ref [37]. In [37], Xu et al. deposited the GO on the broadband mirror as the reflective GOSAs. The saturation intensity of ~108 MW/cm^2 corresponds to the saturation fluence F_{sat} ≈11.9 μJ/cm^2 if recovery time of 110 fs is used [44], which is less than the saturation fluence of 80 μJ/cm^2 in Ref [45], in which the GO were deposited on the quartz using vertical evaporation technique for solid-state laser.

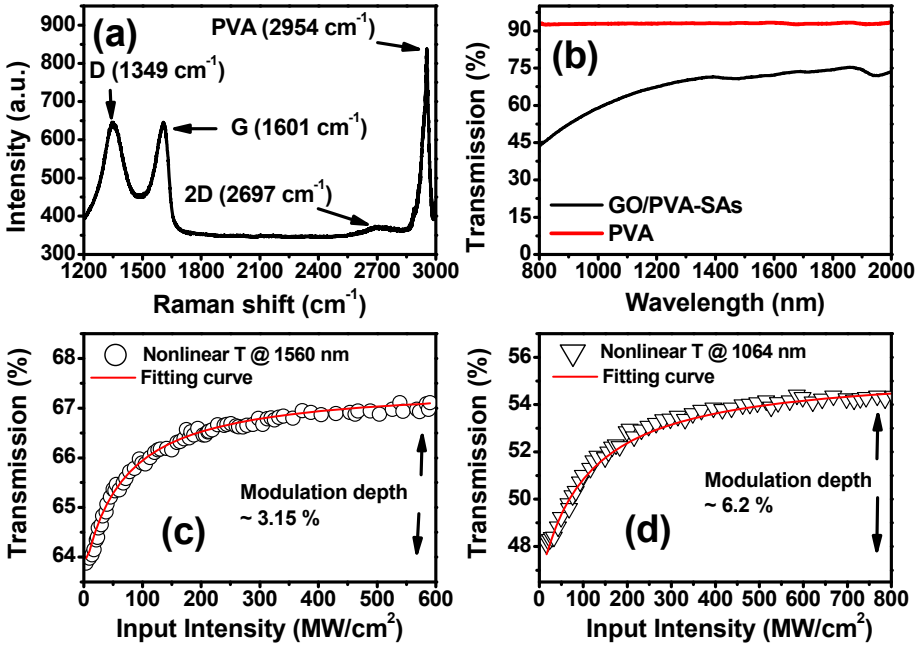

Fig. 1. (a) Raman spectrum measured with 532-nm laser excitation, (b) optical transmission spectra of the GO/PVA-SAs, and nonlinear transmission spectra of the GO/PVA-SAs with excitation wavelength at (c) 1560 nm and (d) 1060 nm. Dots: measured data; solid curve: fitting to the data.

3. Experimental setup of GO mode-locked fiber lasers

The experimental setup of GO passively mode-locked EDFL and YDFL are shown in Fig. 2. The parameters in parentheses are for the YDFL. The laser cavity consists of a 90-cm erbium-doped fiber (ER80-4/125, LIEKKI) (or a 90-cm ytterbium-doped fiber, YB1200-4/125, LIEKKI), a fiber polarization controller, a fiber isolator, a 40% output coupler (30% for YDFL), and a 980/1550 WDM coupler (980/1060 for YDFL). The GOSA was sandwiched between the APC connectors of single-mode fiber jumpers. The gain fiber was core-pumped by a diode laser with center wavelength of 974 nm. The total cavity length is approximately 12.4 m and 20 m for EDFL and YDFL, respectively. The output signals were detected and characterized by a high-speed InGaAs detector, a 500-MHz oscilloscope (LeCroy LT372), a 2.9-GHz radio-frequency (RF) spectrum analyzer (HP 8560E), and an optical spectrum analyzer (Ando AQ6315A). A non-collinear autocorrelator (FR-103WS, Femtochrome Research, Inc.) was used to measure the width of mode-locked pulses.

#208911 - $15.00 USD Received 26 Mar 2014; revised 3 May 2014; accepted 8 May 2014; published 20 May 2014

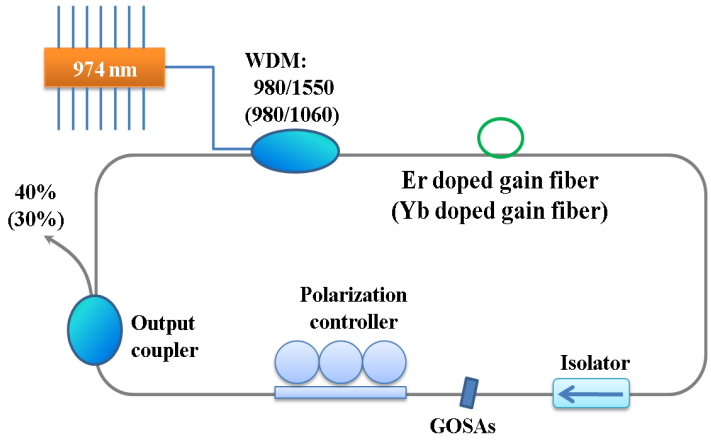

Fig. 2. Schematic setup of GO/PVA-SAs mode-locked fiber lasers

4. Experimental results and discussions

First, the GOSA is inserted into the EDFL. The threshold pump power for continuous-wave lasing is about 37 mW. When the diode pump power increased to 45 mW, self-started mode-locking occurred. Figure 3(a) shows a typical pulse train at 83-mW pumping. The pulse spacing is 62.9 ns, corresponding to the fundamental beating frequency of 15.95 MHz. The RF spectrum is shown in the inset of Fig. 3(a), which shows a very high extinction ratio of 74 dB against noise, indicating good mode-locking stability. We have also measured the mode-locked pulses with autocorrelator and optical spectrum analyzer [Fig. 3(b) and the inset]. By fitting the autocorrelation trace to sech^2 function, the pulse duration was found to be 587 fs. The optical spectrum is centered at 1559.2 nm with a full-width at half-maximum (FWHM) of 5.16 nm and a time-bandwidth product (TBP) of 0.37. Fundamental soliton-like operation was confirmed by the Kelly sidebands of optical spectrum. The laser cavity included 0.9 m of EDF (GVD: 0.021 ps^2/m), 1.85 m of Corning Flexcor 1060 (GVD: –0.007 ps^2/m), and 9.65 m of SMF-28 (GVD: –0.023 ps^2/m). Based on the location of Kelly sidebands, the averaged cavity dispersion was estimated to be 0.1688 ps/nm [52]. Using the measured output power of 2.5 mW, we estimated the pulse energy and peak power to be 0.16 nJ and 267 W, respectively. Further increase of the pump power resulted in wave breaking, and the laser would turn into multi-pulse states.

The identical GO/PVA-SA was then inserted into the YDFL. The laser cavity included 0.9 m of YDF (GVD: 0.027 ps^2/m), 19.1 m of Corning Flexcor 1060 (GVD: 0.029 ps^2/m), and the total dispersion was calculated ~0.578 ps^2 When the diode pump power was increased to 38 mW, CW lasing can be observed. On increasing the pump power to 52 mW, self-started mode locking occurred. Figure 3(c) shows the typical pulse train with repetition rate of 10.05 MHz. The signal-to-noise ratio of 61 dB in the RF spectrum [inset of Fig. 3(c)] indicates good mode-locking stability. The pulse shape of a single pulse is shown as the solid line in Fig. 3(d) by using an oscilloscope (Agilent 86109B). The dashed line is the Gaussian fitting profile, from which the pulse duration of 189 ps is obtained. This result is comparable to Ref [46]. The optical spectrum [inset of Fig. 3(d)] is centered at 1059.7 nm with a full-width at half-maximum of 1.93 nm. The all-normal-dispersion YDFL operates at dissipative soliton (DS) regime, as confirmed by the steep spectral edges in optical spectrum [23]. The TBP is 97, showing that the mode-locked pulses are highly chirped, which is a typical feature of the DSs. It is well known that the highly chirped DS pulses can be compressible outside the cavity. The maximal output power was 12.5 mW at 156 mW pump power, corresponding to single-pulse energy of 1.2 nJ and peak power of 5.91 W. Further increase of the pump power resulted in pulse instability and disappearance of mode-locking. There may be heat accumulated in GO/PVA-SA, leading to pulse instability. However, after decreasing the

#208911 - $15.00 USD Received 26 Mar 2014; revised 3 May 2014; accepted 8 May 2014; published 20 May 2014

pump power, stable self-started mode locking will occur again. Because the DSs are highly chirped, they can also be applied as the input light source in the chirped pulse amplification (CPA) system. By using a double-cladd fiber amplifier, we can easily obtain the output power of 500 mW without pulse breaking. To confirm that mode locking really results from GOSA, we have purposely removed the GO/PVA-SA from the cavity, no mode locking was observed. In this work, the GO/PVA-SA mode-locked YDFL and EDFL can be continuously operated for more than 24 hours.

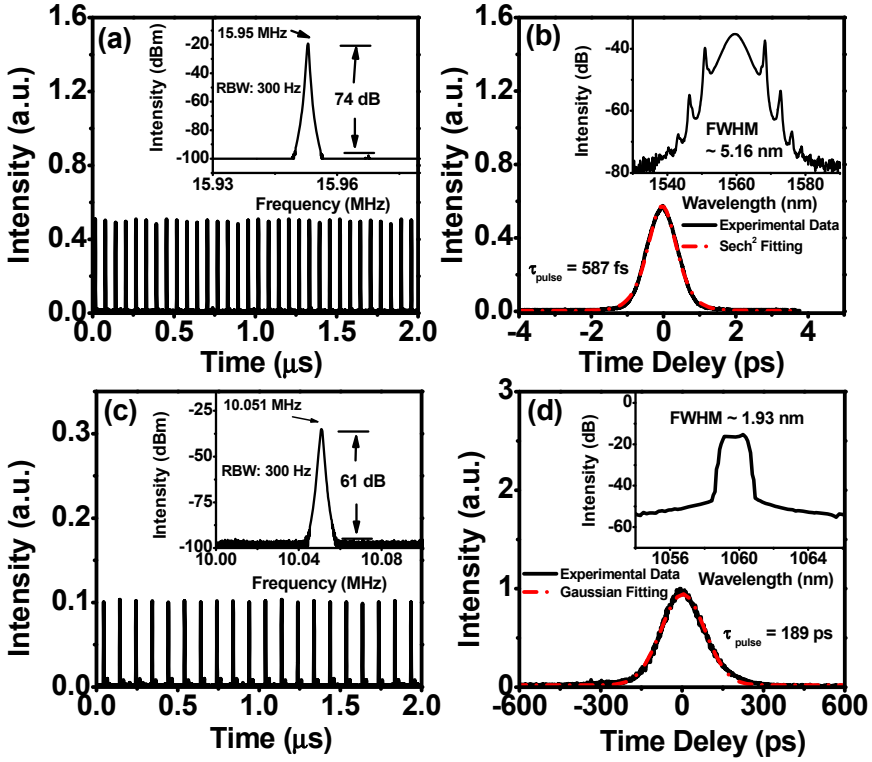

Fig. 3. Pulse train and pulsewidth of GO/PVA-SAs-mode-locked EDFL [(a) and (b)] and YDFL [(c) and (d)]. Insets show the corresponding RF spectrum and optical spectrum.

The bandpass filters can provide the spectral filtering effect for pulse shaping, e.g., an interference filter with 10 nm bandwidth [53], a birefringent filter consisting of a birefringent plate and a polarization beam splitter [54], or a fiber-based Lyot filter with 8.6 nm effective bandwidth [55]. In our YDFL, the DSs can be automatically formed without adding extra filter. The spectral filtering may be provided from intracavity birefringent filter of the laser (an intracavity component with polarization dependent loss and birefringence of intracavity fiber as a Lyot filter) [56], the gain fiber (cutting the pulse temporal wings introduced by normal GVD during intracavity propagation) [57, 58], or the fiber nonlinearity and the chirping induced in the normal-dispersion cavity in conjunction with the nonlinear transmission of GO-SAs [59]. However, the bandwidth of spectral filtering is too wide to effectively shape the pulses.

In order to obtain the few-picosecond or sub-picosecond pulse in all-normal-dispersion YDFL, fiber-based filters with 3-dB spectral bandwidth of about 10 nm, 3 nm and 0.8 nm will be added respectively into the laser cavity. The filter is inserted between GOSAs and polarization controller according to the systematic study by Chong et al. [54] for all-normal-dispersion fiber lasers, where the results show that shortest pulse duration can be obtained after the pulses propagate through the spectral filter. With filter bandwidth of 10 nm and 3 nm, the output pulse duration is almost the same as the previous result of ~189 ps. The

#208911 - $15.00 USD Received 26 Mar 2014; revised 3 May 2014; accepted 8 May 2014; published 20 May 2014

bandwidths of these two filters may be too wide to shape the pulse. Therefore, we spliced a section of 1.5-m polarization maintaining (PM) fiber (PM980, GVD: 0.026 ps^2/m) between the GOSA and polarization controller to obtain an intracavity birefringent filter. When a section of PM fiber (PMF) is introduced into the laser cavity consisting of standard single mode fibers, an intracavity component with polarization dependent loss (PDL) (such as fused fiber coupler or multiplexer etc.) leads to the Lyot filter effect [60]. The total dispersion of this fiber laser was calculated ~0.617 ps^2 with 1.5-m PM fiber. Figures 4(a) and 4(b) show the RF spectrum, optical spectrum, and autocorrelation trace of YDFL with intracavity Lyot filter. When the diode pump power was increased to 40 mW, CW lasing can be observed. After increasing the pump power to 48 mW, self-started mode locking occurred. The typical continuous-wave mode-locking (CWML) pulse train shows the pulse spacing of about 105.2 ns with pump power of ~93 mW, which corresponds to repetition rate of 9.5 MHz and agrees with the RF spectrum in the inset of Fig. 4(a). The pulse train with long time-scale reveals that the CWML state is free of Q-switching modulation. As shown in Fig. 4(a) for fundamental beating frequency of 9.5 MHz, we have demonstrated a clean CWML Yb-doped fiber laser with very high extinction ratio of 68.2 dB against noise, as well as the absence of any spurious modulations. The measured autocorrelation trace of the mode-locked pulses can be well fit to a Gaussian function to obtain FWHM pulsewidth of ~2.73 ps [Fig. 4(b)] with optical spectrum centered at 1057.2 nm and spectral width of 0.75 nm [inset of Fig. 4(b)]. The time-bandwidth product is about 0.547, which is slightly larger than the transform-limited value of 0.44 for Gaussian pulses, indicating that the mode-locked pulses are chirped and their duration could be further narrowed. To our best knowledge, this is the shortest pulse duration directly obtained from an all-normal-dispersion YDFL with GOSAs. For a birefringent fiber filter, the wavelength spacing ($\Delta\lambda$) between two neighboring spectral peaks can be decided by the formula $\lambda^2/(\Delta n \cdot L)$ [61], where λ, Δn, and L are the laser wavelength, birefringence of the PMF, and length of PMF, respectively. When the values of λ, Δn, and L were used (1057.2 nm, 4.0×10^{-4}, and 1.5 m, respectively), $\Delta\lambda$ is calculated to be 1.87 nm, which is close to the measured result (~1.7 nm) in the inset of Fig. 4(b). In use of the measured average output power of 2.1 mW, repetition rate of 9.5 MHz, and pulsewidth of 2.73 ps, the pulse energy and peak power are estimated to be 0.22 nJ and 81.8 W, respectively at 93 mW pumping.

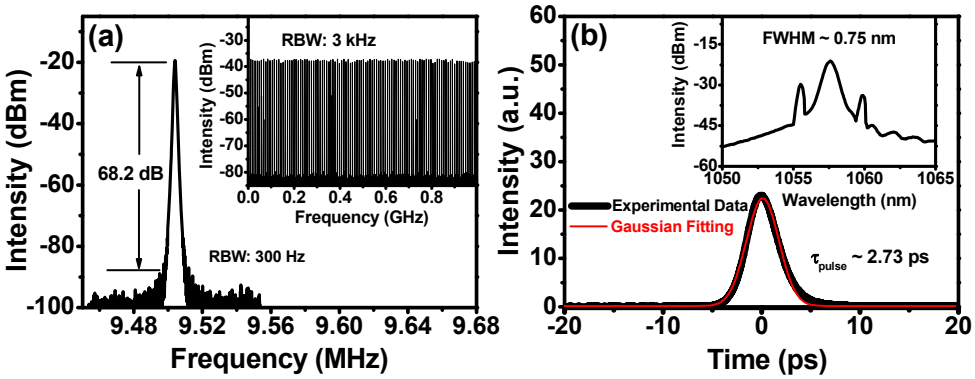

Fig. 4. (a) Radio frequency spectrum (first beat note). Inset: the radio frequency spectrum for 1-GHz scan range. (b) The measured autocorrelation trace (black line) and Gaussian function fitting (red line). The inset shows the output spectrum of the GOSA mode-locked ytterbium-doped fiber laser.

5. Conclusion

We have fabricated graphene oxide/PVA saturable absorbers, and the modulation depths of GO/PVA-SA are 3.15% and 6.2% at 1.06 μm and 1.55 μm, respectively. Stable and self-starting passively mode-locked YDFL and EDFL are demonstrated utilizing this absorber.

#208911 - $15.00 USD Received 26 Mar 2014; revised 3 May 2014; accepted 8 May 2014; published 20 May 2014

The mode-locked EDFL is implemented with a total cavity length of 12.4 m and 40% output, for which the spectral width, repetition rate, and pulse duration are 5.16 nm, 15.9 MHz, and 587 fs, respectively. Using the same GOSA for YDFL mode-locking, 10.05-MHz repetition rate, 189-ps pulse duration and output power of 12.5 mW have been obtained with cavity length of about 20 m. It is revealed that a GOSA can be used in both EDFL and YDFL to obtain stable and self-starting mode-locked laser pulses. Finally, a birefringent filter is inserted into the YDFL cavity. Spectral width, repetition rate, and pulse duration of 0.75 nm, 9.5 MHz, and 2.7 ps have been obtained. This is the shortest pulse duration directly obtained from an all-normal-dispersion YDFL with GOSAs, which is an improvement on the previous report of 191 ps.

Acknowledgment

This work is supported by the Ministry of Science and Technology of Taiwan, Republic of China, under grants NSC 102-2112-M-009-016-MY3, and NSC 101-2221-E-845-001-MY3.

#208911 - $15.00 USD Received 26 Mar 2014; revised 3 May 2014; accepted 8 May 2014; published 20 May 2014